

# Topologically Matching Supramolecular n/p-Heterojunction Architectures\*\*

Rajesh Bhosale, Alejandro Perez-Velasco, Velayutham Ravikumar, Ravuri S. K. Kishore, Oksana Kel, Alberto Gomez-Casado, Pascal Jonkheijm, Jurriaan Huskens, Plinio Maroni, Michal Borkovec, Tomohisa Sawada, Eric Vauthey,\* Naomi Sakai,\* and Stefan Matile\*

Directional energy, electron, and hole transport along sophisticated redox/energy gradients to and from active site is essential in photosynthesis.<sup>[1]</sup> Applied to molecular optoelectronics, such as bulk n/p-heterojunction (BHJ) organic solar cells,<sup>[2,3]</sup> these lessons from nature<sup>[4]</sup> call for systems in which *n*- and *p*-semiconducting pathways are aligned coaxially at the molecular level. These supramolecular n/p-heterojunctions (SHJs) will have to contain judiciously placed chromophores of different color and with different redox properties to absorb as much light as possible and rapidly move the generated electrons and holes in opposite directions. Supramolecular chemistry approaches appear to be perfect for creating such SHJs with oriented multicolored antiparallel redox gradients (OMARGs). However, reliable bottom-up routes toward OMARG-SHJs do not exist to date, despite efforts by many groups.<sup>[5–22]</sup> We have considered the zipper

assembly of naphthalenediimide (NDI)  $\pi$  stacks along *p*-oligophenyl (POP) scaffolds to construct the surface architectures needed to tackle this challenge.<sup>[20–22]</sup> Herein, we introduce oligophenylethynyl (OPE) scaffolds to explore the importance of topological matching for zipper architectures and to determine the compatibility of zipper assembly with the creation of OMARG-SHJs.

In zipper assembly,<sup>[20,21]</sup> NDI chromophores attached to rigid-rod scaffolds are assembled step-by-step to build mutually interdigitating  $\pi$  stacks along interdigitating rigid-rod scaffolds, which should serve as hole ( $h^+$ ) and electron ( $e^-$ ) transporting pathways, respectively. NDIs were selected as  $\pi$  stacks in zipper assembly because they unify favorable properties, such as 1) availability in all colors, 2) decreasing HOMO/LUMO levels with increasing bandgap (Figure 1), 3) *n*-semiconductivity, 4)  $\pi$  acidity, 5) planarity, 6) global structural preservation, 7) compactness (“atom efficiency”), and 8) synthetic accessibility.<sup>[19–26]</sup>

[\*] O. Kel, Prof. E. Vauthey  
Department of Physical Chemistry, University of Geneva  
Geneva (Switzerland)  
E-mail: eric.vauthey@unige.ch

R. Bhosale, Dr. A. Perez-Velasco, Dr. V. Ravikumar,  
Dr. R. S. K. Kishore, Dr. N. Sakai, Prof. S. Matile  
Department of Organic Chemistry, University of Geneva  
Geneva (Switzerland)  
Fax: (+41) 22-379-3215  
http://www.unige.ch/sciences/chior/matile/  
E-mail: naomi.sakai@unige.ch  
stefan.matile@unige.ch

A. Gomez-Casado, Dr. P. Jonkheijm, Prof. J. Huskens  
Molecular Nanofabrication Group, University of Twente  
Enschede (The Netherlands)

Dr. P. Maroni, Prof. M. Borkovec  
Department of Inorganic and Analytical Chemistry, University of Geneva  
Geneva (Switzerland)

T. Sawada  
Department of Applied Chemistry, School of Engineering, University of Tokyo  
Tokyo (Japan)

[\*\*] We thank D.-H. Tran, L. Maffiolo, and S. Maity for contributions to synthesis, D. Jeannerat, A. Pinto, and S. Grass for NMR spectroscopy measurements, P. Perrotet, N. Oudry, and G. Hopfgartner for mass spectrometry, and the University of Geneva, the GCOE program of the University of Tokyo (T.S.), the nanotechnology network Nanoned (J.H., P.J.), and the Swiss NSF (S.M., E.V., M.B.) for financial support.

Supporting information for this article is available on the WWW under <http://dx.doi.org/10.1002/ange.200902551>.

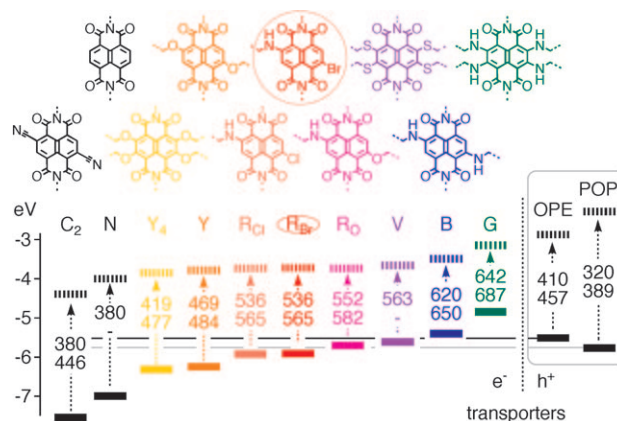


**Figure 1.** Building blocks for OMARG-SHJ photosystems. Frontier orbital energy levels of NDIs (C<sub>2</sub>–G), POPs, and OPEs (solid lines, HOMO; dashed lines, LUMO; dashed arrows, absorption of light ( $h\nu$ ); with wavelength (nm) of maximal absorption (top) and emission (bottom). Data from references [19, 22, 25, 26] and herein).

POPs are however not perfect for zipper assembly because their repeat distance (about 10 Å) exceeds the repeat of face-to-face  $\pi$  stacks ( $2 \times$  circa 3.5 Å; Figure 2).<sup>[23]</sup> In contrast to POPs, OPEs have perfect repeats (circa 7 Å) for  $\pi$ -stacking architectures. Moreover, OPEs are planarizable,<sup>[27,28]</sup> better and red-shifted fluorophores,<sup>[17]</sup> better hole

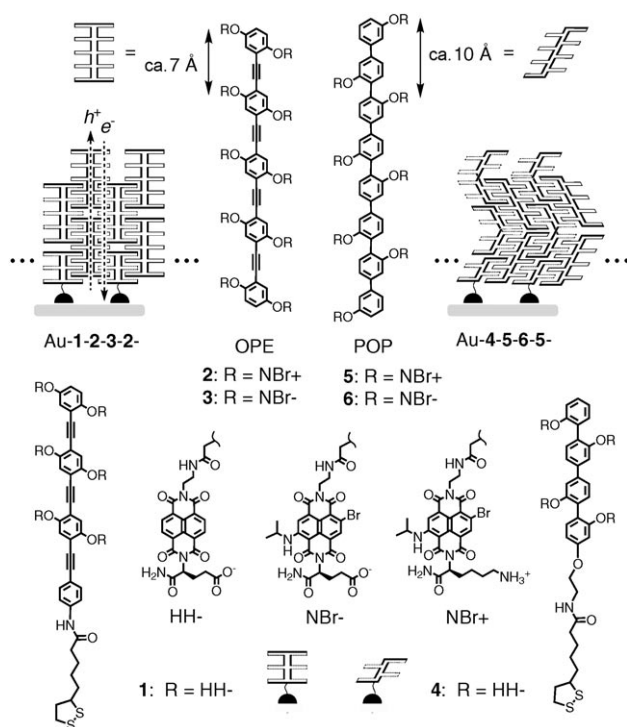


**Figure 2.** Molecular structures and supramolecular architectures of OPE-NDI and POP-NDI initiators (**1/4**) and propagators (**2,3/5,6**) and of their matched and mismatched zipper assembly Au-1-2-3-2- and Au-4-5-6-5-, respectively.

conductors,<sup>[28,29]</sup> and better electron donors (Figure 1; Supporting Information, Figure S3, Table S1).

OPE-NDI dyads **1–3** and POP-NDI dyads **4–6** were prepared by multistep syntheses (Figure 2; Supporting Information, Schemes S1–8).<sup>[30]</sup> Zipper assembly of OPE-NDI architectures Au-1(-2-3)<sub>n</sub> was initiated by deposition of the short initiator **1** on gold electrodes. The obtained Au-**1** was

then dipped into an aqueous solution of the OPE propagator **2**. The lower half of the red and cationic NDIs of **2** were expected to  $\pi$ -stack with the colorless and anionic NDI acceptors of **1**, whereas the upper half remains free as a “sticky end” to zip up with anionic OPE propagator **3**, which in turn can zip up with cationic **2**, and so on. Zipper assembly of OPE-NDI systems Au-1(-2-3)<sub>n</sub> depends on factors such as concentration, solvents, ionic strength, incubation time, temperature, and sample freshness. Vigorous optimization revealed incubation with 5–10  $\mu$ M solutions of **2** or **3** in 50% aqueous trifluoroethanol (TFE) with 1M NaCl and 0.5 mM pH 7 phosphate buffer for 1–2 days at ambient temperature as the best conditions (Supporting Information, Figures S4,8). POP-NDI systems Au-4(-5-6)<sub>n</sub> were zipped-up under similar conditions.

OPE-NDI architectures Au-1(-2-3)<sub>n</sub> were characterized by photocurrent generation with 50 mM triethanolamine (TEOA, pH 10) in 100 mM aqueous Na<sub>2</sub>SO<sub>4</sub> as electron donor and a platinum electrode as cathode (Supporting Information, Figures S5,6). Upon deposition of layers, photocurrent densities increased almost linearly until reaching saturation at about 20 layers, that is, Au-1(-2-3)<sub>10</sub> (Figure 3a,  $\circ$ ). POP-NDI architectures approached saturation at about 10 layers, that is, Au-4(-5-6)<sub>5</sub>, and generated 40% less photocurrent (Figure 3b,  $\circ$ ).

OPE-NDI zippers Au-1-2 were incubated with **1** to cap the sticky ends and terminate zipper growth. Repeated incubation of Au-1-2-1 with **2** and **3** did not increase the photocurrent (Figure 3a,  $\bullet$ ). Capping of Au-4-5 did not terminate the POP-NDI “zippers” Au-4-5-4 (Figure 3b,  $\bullet$ ). This insensitivity of POP-NDI zippers to capping occurred with halogenated NDIs only; blue POP-NDI zippers with alkylamino substituents responded correctly to capping.<sup>[20]</sup>

To compare zipper assembly with the conventional layer-by-layer (LBL) assembly, gold electrodes were covered with liponic acid **7** in place of initiators **1** or **4**. This comparison is demanding because extensive experience with the more

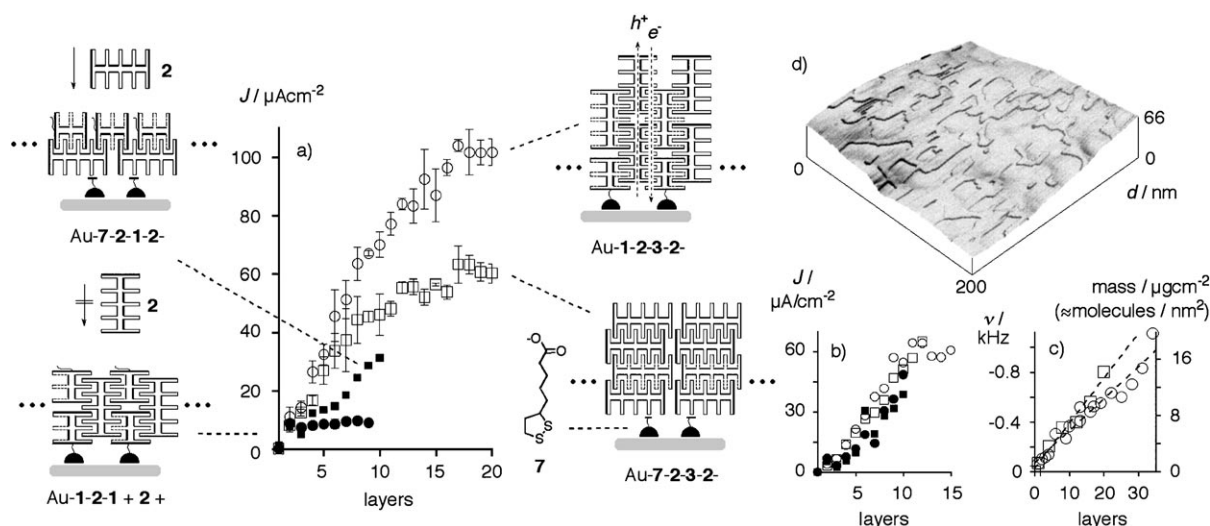


**Figure 3.** Characteristics of OPE-NDI architectures (a,c,d) compared to POP-NDI controls (b). Photocurrent densities (a,b) and QCM frequencies (c, with linear curve fit) as a function of the number of theoretical layers of zipper ( $\circ$ ,  $\bullet$ ) or LBL assembly ( $\square$ ,  $\blacksquare$ ) without ( $\circ$ ,  $\square$ ) or with ( $\bullet$ ,  $\blacksquare$ ) capping. d) Tapping-mode 3D AFM height profile of Au-1(-2-3)<sub>16</sub>-2.

“fuzzily”<sup>[16]</sup> organized LBL assembly<sup>[14,15]</sup> leaves no doubt that the anionic Au-7 will ion-pair with the cationic OPE-NDI **2**, cationic Au-7-2 will ion-pair with the anionic OPE-NDI **3**, and so on (Figure 3). Photocurrent density saturated at about 8 layers with OPE-NDI architectures generated LBL, whereas zipper saturation occurs at 20 layers (Figure 3a,  $\circ$  versus  $\square$ ). The maximal short-circuit current of Au-7(-2-3)<sub>n</sub> was half of that generated by Au-1(-2-3)<sub>10</sub>. LBL assembly should be irresponsive to capping because any eventual OPE interdigitation is functionally irrelevant. This is exactly what was found for the LBL assembly of OPE-NDI dyads, that is, Au-7-2-1(-2-3)<sub>n</sub> (Figure 3a,  $\blacksquare$ ). Mismatched POP-NDI architectures were not only irresponsive to different modes of assembly but also to all capping experiments (Figure 3b).

The mass deposited per layer was determined electro-mechanically with a quartz crystal microbalance (QCM) (Figure 3c). Equal quantities were found to deposit for zipper and LBL assembly without saturation. This suggested that photocurrent saturation occurs because charges start to recombine before reaching the electrodes, and not because the growth of the assembly stops. The observed “critical thickness” thus relates to charge mobility; that is, supramolecular organization. Better critical thickness of OPE zippers (about 20 layers) compared to LBL assemblies (circa 10 layers) and POP zippers (circa 8 layers) is thus consistent with the long-range organization of topologically matching OPE-NDI zipper architectures (Figure 3).

Excellent organization of OPE-NDI zipper architectures was confirmed with smooth surfaces in atomic force microscopy (AFM) images (Figure 3d), smoother than those of LBL and POP controls (Supporting Information, Figures S9–11) as well as LBL and BHJ photosystems in the literature.<sup>[3,8,14]</sup> Different to LBL<sup>[14]</sup> and related approaches,<sup>[8]</sup> surface roughness did not significantly increase with multilayer thickness. AFM images further revealed steps of 1.5 nm height as expected for zipper assembly, and occasional clumps of unknown origin but seen already for Au-1. Access to low surface roughness has been proposed to be important in molecular optoelectronics, including high photovoltaic efficiency.<sup>[3]</sup> Indeed, current–voltage curves of OPE-NDI zippers Au-1(-2-3)<sub>7</sub> revealed a fill factor (FF) of 61 % (Supporting Information, Figure S7). As in the thick films prepared “top-down” in optimized BHJ organic solar cells,<sup>[3]</sup> this FF was consistent with high charge mobility in OPE-NDI architectures. When considering plasmon resonance quenching on gold by factors up to 280, the reported short circuit currents are quite high.<sup>[18]</sup>

The action spectrum of OPE-NDI zipper Au-1(-2-3)<sub>7</sub> revealed that this photoactivity is due not only to organization but also to the contribution of both NDIs and OPEs to the light harvesting (Figure 4b,  $\bullet$ ). Moreover, the observed bathochromic absorption of OPE in the action spectrum implies co-planar orientation of phenyl groups. OPE planarization was expected for the zipper architecture, and should give rise to higher charge mobility of the *p*-semiconductor.<sup>[27,28]</sup>

Femtosecond fluorescence and transient absorption spectroscopy provided further support for the high photoactivity of OPEs (Figure 4a; Supporting Information, Figures S17–

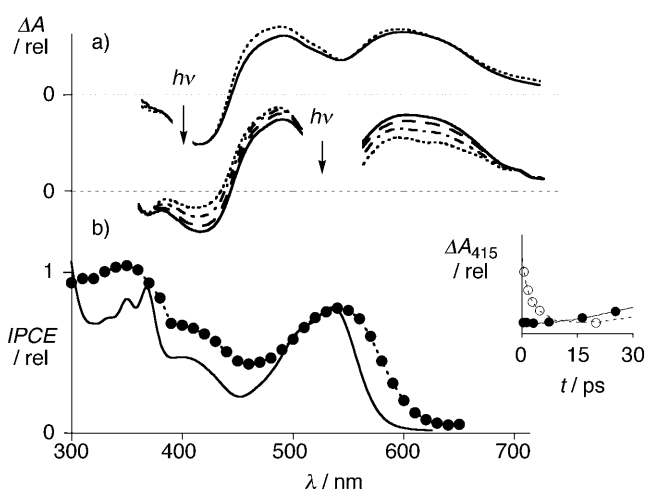


**Figure 4.** Transient absorption and action spectra of OPE-POP systems. a) Transient absorption spectra recorded 0.8 (dotted) and 10 ps (solid) after excitation of OPE-NDI **2** at 400 nm (top) and 0.1 (dotted), 1, 3.5 and 10 ps (solid) after excitation of **2** at 520 nm (bottom); inset:  $\Delta A$  at 415 nm with time after excitation at 400 ( $\bullet$ ) and 520 nm ( $\circ$ ). b) Action spectrum of OPE-NDI zipper Au-1(-2-3)<sub>7</sub> ( $\bullet$ ) compared to absorption spectra of **2** in methanol with 2% triethylamine (solid line).

22). The appearance of OPE bleaching at 415 nm together with the broad NDI radical anion band around 600 nm indicated that, independent of the initially excited chromophore, very fast electron transfer takes place from OPE to NDI, and that the formed charge separated state (OPE<sup>+</sup>–NDI<sup>•−</sup> pair) of **2** is relatively long-lived (flash photolysis lifetime  $\tau_4$  = 270 ns; Supporting Information, Table S4). This finding was important as it demonstrates the presence of the OPE<sup>+</sup>–NDI<sup>•−</sup> pair; that is, supramolecular n/p-heterojunctions. The faster charge separation observed upon OPE excitation than upon NDI excitation further demonstrated that electron rather than energy transfers from OPE to NDI (Figure 4a and inset). For POP-NDI, both photoinduced charge separation and charge recombination were slower and influenced by unusual and more complex triplet contributions arising from heavy-atom effects (lifetime  $\tau_4$  = 2.5  $\mu$ s; Supporting Information, Table S4).

In summary, we report synthetic access to ordered, oriented multicomponent surface architectures, and that topological matching is the key to get there. The obtained photosystems excel with efficient photocurrent generation, smooth surfaces, and perfect responsiveness to functional probes for the existence of operational intra- and interlayer recognition motifs. Homologous photosystems with mismatched POP scaffolds or “fuzzy”<sup>[16]</sup> organizations made by standard layer-by-layer assembly are less functional. These results demonstrate that highly ordered and oriented supramolecular organization is achievable only through careful design, and that it matters for function. Access to surface architectures with long-range organization will be essential for future molecular optoelectronics, including OMARG-SHJ solar cells or molecular logic devices.

Received: May 13, 2009  
Published online: July 27, 2009

**Keywords:** optoelectronics · photocurrents · photosynthesis · solar energy · supramolecular chemistry

- [1] J. Deisenhofer, H. Michel, *Science* **1989**, *245*, 1463–1473.
- [2] G. Yu, J. Gao, J. C. Hummelen, F. Wudl, A. J. Heeger, *Science* **1995**, *270*, 1789–1791.
- [3] B. C. Thompson, J. M. J. Fréchet, *Angew. Chem.* **2008**, *120*, 62–82; *Angew. Chem. Int. Ed.* **2008**, *47*, 58–77.
- [4] D. A. LaVan, J. N. Cha, *Proc. Natl. Acad. Sci. USA* **2006**, *103*, 5251–5255.
- [5] T. van der Boom, R. T. Hayes, Y. Zhao, P. J. Bushard, E. A. Weiss, M. R. Wasielewski, *J. Am. Chem. Soc.* **2002**, *124*, 9582–9590.
- [6] F. Würthner, Z. Chen, F. J. M. Hoeben, P. Osswald, C.-C. You, P. Jonkhøj, J. Herrikhuyzen, A. P. H. J. Schenning, P. P. A. M. van der Schoot, E. W. Meijer, E. H. A. Beckers, S. C. J. Meskers, R. A. J. Janssen, *J. Am. Chem. Soc.* **2004**, *126*, 10611–10618.
- [7] Y. Yamamoto, T. Fukushima, Y. Suna, N. Ishii, A. Saeki, S. Seki, S. Tagawa, M. Taniguchi, T. Kawai, T. Aida, *Science* **2006**, *314*, 1761–1764.
- [8] A. Kira, T. Umeyama, Y. Matano, K. Yoshida, S. Isoda, J. K. Park, D. Kim, H. Imahori, *J. Am. Chem. Soc.* **2009**, *131*, 3198–3200.
- [9] D. M. Guldi, *J. Phys. Chem. B* **2005**, *109*, 11432–11441.
- [10] A. B. F. Martinson, A. M. Massari, S. J. Lee, R. W. Gurney, K. E. Splan, J. T. Hupp, S. T. Nguyen, *J. Electrochem. Soc.* **2006**, *153*, A527–A532.
- [11] M. Morisue, S. Yamatsu, N. Haruta, Y. Kobuke, *Chem. Eur. J.* **2005**, *11*, 5563–5574.
- [12] C.-H. Huang, N. D. McClenaghan, A. Kuhn, G. Bravic, D. M. Bassani, *Tetrahedron* **2006**, *62*, 2050–2059.
- [13] H. J. Snaith, G. L. Whiting, B. Sun, N. C. Greenham, W. T. S. Huck, R. H. Friend, *Nano Lett.* **2005**, *5*, 1653–1657.
- [14] L. Zhao, T. Ma, H. Bai, G. Lu, C. Li, G. Shi, *Langmuir* **2008**, *24*, 4380–4387.
- [15] J. K. Mwaura, M. R. Pinto, D. Witker, N. Ananthakrishnan, K. S. Schanze, J. R. Reynolds, *Langmuir* **2005**, *21*, 10119–10126.
- [16] G. Decher, *Science* **1997**, *277*, 1232–1237.
- [17] J. N. Clifford, T. Gu, J.-F. Nierengarten, N. Armaroli, *Photochem. Photobiol. Sci.* **2006**, *5*, 1165–1172.
- [18] H. Yamada, H. Imahori, Y. Nishimura, I. Yamazaki, T. K. Ahn, S. K. Kim, D. Kim, S. Fukuzumi, *J. Am. Chem. Soc.* **2003**, *125*, 9129–9139.
- [19] B. A. Jones, A. Facchetti, M. R. Wasielewski, T. J. Marks, *J. Am. Chem. Soc.* **2007**, *129*, 15259–15278.
- [20] N. Sakai, A. L. Sisson, T. Bürgi, S. Matile, *J. Am. Chem. Soc.* **2007**, *129*, 15758–15759.
- [21] A. L. Sisson, N. Sakai, N. Banerji, A. Fürstenberg, E. Vauthey, S. Matile, *Angew. Chem.* **2008**, *120*, 3787–3789; *Angew. Chem. Int. Ed.* **2008**, *47*, 3727–3729.
- [22] N. Sakai, R. S. K. Kishore, S. Matile, *Org. Biomol. Chem.* **2008**, *6*, 3970–3976.
- [23] S. Bhosale, A. L. Sisson, P. Talukdar, A. Fürstenberg, N. Banerji, E. Vauthey, G. Bollot, J. Mareda, C. Röger, F. Würthner, N. Sakai, S. Matile, *Science* **2006**, *313*, 84–86.
- [24] H. Yan, Z. Chen, Y. Zheng, C. Newman, J. R. Quinn, F. Dötz, M. Kastler, A. Facchetti, *Nature* **2009**, *457*, 679–686.
- [25] F. Würthner, S. Ahmed, C. Thalacker, T. Debaerdemaeker, *Chem. Eur. J.* **2002**, *8*, 4742–4750.
- [26] C. Röger, F. Würthner, *J. Org. Chem.* **2007**, *72*, 8070–8075.
- [27] W. Hu, N. Zhu, W. Tang, D. Zhao, *Org. Lett.* **2008**, *10*, 2669–2672.
- [28] S. B. Sachs, S. P. Dudek, R. P. Hsung, L. R. Sita, J. F. Smalley, M. D. Newton, S. W. Feldberg, C. E. D. Chidsey, *J. Am. Chem. Soc.* **1997**, *119*, 10563–10564.
- [29] B. Albinsson, M. P. Eng, K. Pettersson, M. U. Winters, *Phys. Chem. Chem. Phys.* **2007**, *9*, 5847–5864.
- [30] See the Supporting Information.